



Research article

Synthesis of Cu and Zr-based coordination polymers with N/O donors and investigation of their photocatalytic activity against dye

Md Mohibul Alam^a, Md. Foysal Ahmed^a, Md. Azharul Arafath^{b,*},
Mohammad Razaul Karim^b, Md Nizam Uddin^b, Md Sohrab Hossain^c

^a Department of Chemical Engineering & Polymer Science, Shahjalal University of Science and Technology, Sylhet 3114, Bangladesh

^b Department of Chemistry, Shahjalal University of Science and Technology, Sylhet 3114, Bangladesh

^c HiCoE-Centre for Biofuel and Biochemical Research, Institute of Sustainable Energy, Department of Fundamental and Applied Sciences, Faculty of Science and Information Technology, Universiti Teknologi PETRONAS, Seri Iskandar 32610, Perak Darul Ridzuan, Malaysia

ARTICLE INFO

Keywords:

Coordination polymer
Photocatalysis
Powder-XRD
SEM
Methylene blue

ABSTRACT

The coordination polymers (CPs) of Cu and Zr were synthesized by the hydrothermal method. The otrotic acid potassium salt (H_3KL) was used as a linker, which coordinates via O–O. Whereas, 4,4'-trimethylenedipyridine (4,4'-TMDP) was used as a bifunctional monomer, which coordinates via N–N. The synthesized CPs were characterized by FTIR, P-XRD, TGA, DSC and SEM. The photocatalytic activity was investigated against methylene blue (MB) under sunlight irradiation. Both Cu-CP and Zr-CP exhibited potential activity for the degradation of MB, which was 72 % for Cu-CP and 93 % for Zr-CP. The band gap of the CPs was also investigated, and the observed value was 2.2 eV. The band gap indicates that these compounds could bring breakthroughs as photocatalysts instead of semiconductors. These kinds of CPs could be used for multiple purposes in industry and in a green environment.

1. Introduction

In the last few decades, industrialization has not only vastly improved our living standards, but it has also increased the number of inorganic and organic pollutants that threaten the environment and individual health [1]. Paper, plastics, rubber, coatings, and organic dyes are widely used in textile as vital industrial components. The elimination of these hazardous substances prior to their release into the natural system is a crucial issue from an environmental standpoint [2–4]. Nearly all dyes are lethal and cause severe problems to the environment, humans and animals. It is necessary to have a practicable and cost-effective method for removing these pigment molecule from effluents in order to reduce their potential toxicity. The removal of pollutants and organic dyes from water can be accomplished using a variety of processes, such as adsorption [5,6] using porous materials, flocculation, biological processes, membranes, precipitation, and others. However, these processes typically suffer from huge costs, low efficiency, and the generation of secondary pollutants. Therefore, it is imperative to develop effective methods and techniques for purifying the wastewater. Photocatalytic degradation has become one of the most effective methods for removing dyes in ambient conditions with an environmentally friendly photocatalyst. These materials and photocatalytic technique are feasible in terms of cost, operation, stability, and efficiency.

* Corresponding author.

E-mail addresses: arafath-che@sust.edu, arafath.usm@gmail.com (Md.A. Arafath).

In recent years, coordination polymers (CPs), also known as metal–organic frameworks, have garnered a lot of attention due to a wide variety of configurations they may take and the possible applications they might have. Rapid developments and appealing applications in fluorescence sensing [7,8], gas absorption [9,10], molecular magnetism [11,12], molecular storage [13–15], drug-delivery [16,17], supercapacitor [18], and heterogeneous catalysis [19–21] have resulted from their assembly from well-customized links with organic ligands and inorganic metal/metal nodes. Photocatalysis is a newly developing application for CPs, and some experiments have shown that CPs are effective photocatalysts for the degradation of organic dyes [22,23]. It's has diversity for bonding of metal center to photoactive organic ligands. The synthesized CPs for the required purposes of photodegradation could be efficient photocatalysts when subjected to irradiation from various light sources. When compared to conventional inorganic semiconductors, these extended CPs have a number of inherent benefits including improved solar energy utilization, zero secondary pollution, improved ease of modification, and long-term durability, which ensure their widespread application as photocatalysts for the production of high-quality reclaimed water in the context of environmental remediation. In this investigation, Zr and Cu-based CPs were synthesized in which orotic acid potassium salt (H_3KL) and 4,4'-trimethylenedipyridine (4,4'-TMDP) were utilized as O donors and N donors, respectively.

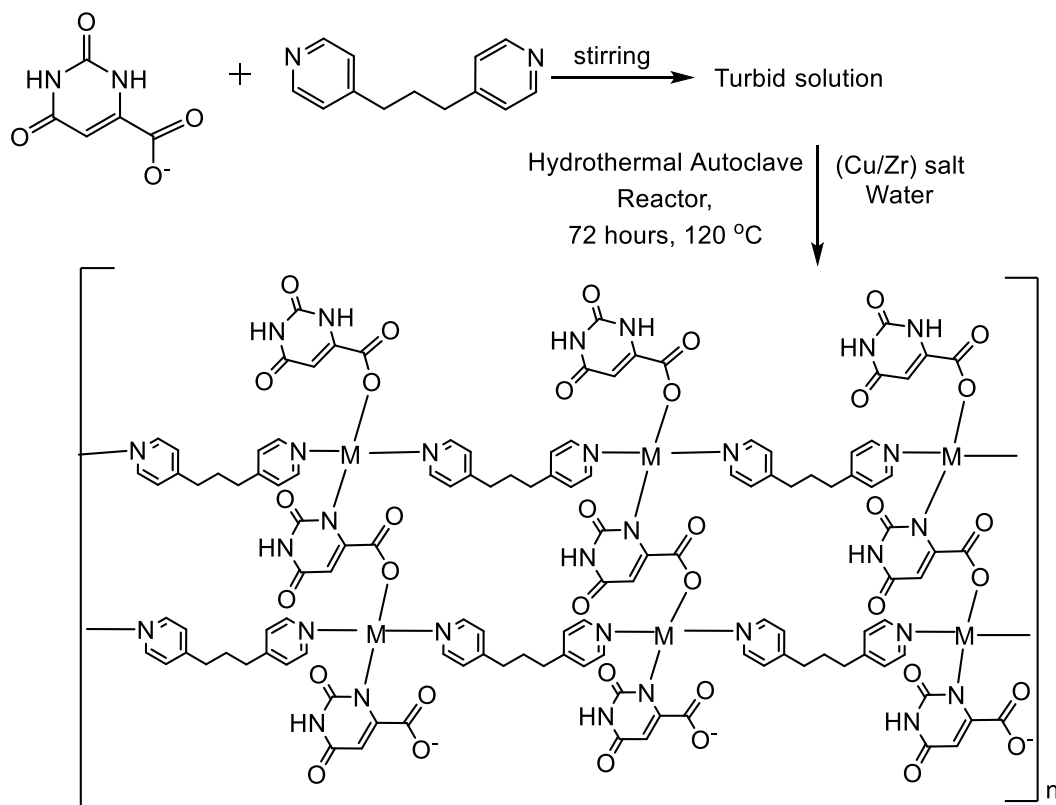
2. Materials and method

2.1. Materials

The chemicals used in this study were commercially available and utilized without undergoing any purification process. Zirconium Oxychloride and Cupric Chloride were procured from Qualikems, while H_3KL and 4,4'-TMDP were procured from Sigma–Aldrich Co. Ltd.

2.2. Methods

The FTIR spectra in the $400\text{--}4000\text{ cm}^{-1}$ region was acquired using KBr pellets and an IRPrestige-21 instrument from Shimadzu Corporation. A thermal analysis was conducted utilizing the TGA-50H, Shimadzu Corporation instrument, with a heating rate of $10\text{ }^\circ\text{C}/\text{min}$, over a temperature range of $25\text{--}1200\text{ }^\circ\text{C}$. PXRD analysis was used to arrive at a conclusion on the crystallinity of the CPs by utilizing the SmartLab X-ray diffractometer, a Rigaku Corporation instrument. The morphology and microstructures were determined



Scheme 1. The scheme shows the synthesis route of coordination polymer of Zr^{2+} (Zr-CP) and Cu^{2+} (Cu-CP).

using Scanning Electron Microscopy (SEM) EVO 18 Carl Zeiss AG of UK.

2.2.1. Synthesis of coordination polymer of Zr (Zr-CP)

A solution was prepared by combining 1 mmol (0.19826g) of 4,4'-TMDP and 1 mmol (0.19419g) of H₃KL in a beaker containing 50 mL of water. The solution was agitated for a duration of 40 min at ambient temperature. Subsequently, a quantity of 2 mmol (0.6445g) of Zirconium oxychloride was introduced into the aforementioned mixture, which was then subjected to stirring for a duration of 20 min (Scheme 1). Subsequently, the solution was relocated to be hydrothermally enclosed within a Teflon-lined reactor with a volume of 100 mL and subjected to a temperature of 120 °C for a duration of 72 h. The almost white crystal product was obtained by cooling the reactor at a rate of 5 °C per minute, and then the product was washed and dried, respectively.

2.2.2. Synthesis of coordination polymer of Cu (Cu-CP)

A solution was prepared by combining 1 mmol (0.19826 g) of 4,4'-TMDP and 1 mmol (0.19419 g) of H₃KL in a beaker containing 50 mL of water. The solution was agitated for a duration of 40 min at ambient temperature. Subsequently, a quantity of 2 mmol (0.34056 g) of cupric chloride was introduced into the aforementioned mixture, which was then subjected to stirring for a duration of 20 min (Scheme 1). Subsequently, the solution was relocated to be hydrothermally enclosed within a Teflon-lined reactor with a volume of 100 mL and subjected to a temperature of 120 °C for a duration of 72 h. The saddle brown crystal product was obtained by cooling the reactor at a rate of 5 °C per minute, and then the product was washed and dried, respectively.

2.2.3. Synthetic strategy and structural description of CPs

It is necessary to discuss the structure of the ligands in order to find the structure of the two coordination polymers. In the structure of H₃KL, there are three strong coordination sites shown in Scheme 2(a), each of which is capable of forming a bond with a metal (M). Furthermore, this structure is not symmetrical in its very makeup. Additionally, 4,4'-TMDP has two powerful coordination sites shown in Scheme 2(b) that may be used in the process of bonding with M. 4,4'-TMDP was handled as a ligand, and it was metal that was used to propagate it in a one-dimensional (1D) fashion. Meanwhile, H₃KL was handled as a linker, and it was utilized to connect that 1D chain to another 1D chain in order to create it as a 2D structure. Moreover, two identical 2D structures can combine to make a 3D structure.

2.2.4. Photodegradation of methylene blue (MB)

Initially, the pH effect was tested at different concentrations to get optimum pH for degradation. The solution of MB of different concentrations in the range of 4–10 ppm was prepared for the investigation of degradation. In the solution of MB at different pH the CPs catalyst was added, then it was placed under sunlight, and different samples were collected at a constant time interval (15 min) over the time to measure the degradation using the catalysts. For the dark condition, the same solution with photocatalyst was placed in the dark for 1 h at pH 9.2. and samples were collected at different times with a constant time interval (15 min). The MB was also placed under sunlight without a catalyst for comparing the efficiency of the catalysts. Finally, the absorbances of these samples were measured by LAMBDA 365+ UV/Vis Spectrophotometer, a PerkinElmer Corporation instrument. The concentrations were determined using calibration curve from the recorded absorbances. Finally, the percentage of degradation was calculated using the formula:

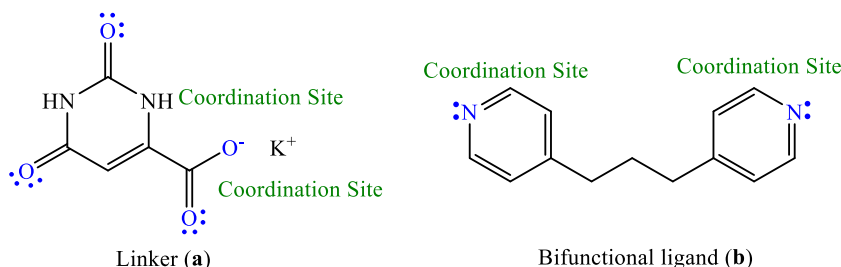
$$\text{Degradation} = \frac{C_0 - C_t}{C_0} \times 100\% = \frac{A_0 - A_t}{A_0} \times 100\%$$

C₀ = Initial concentration; C_t = concentration at time t.

A₀ = Initial absorbance of solution; A_t = Absorbance of solution at time t.

2.2.5. Band gap measurement

The optical band gap was figured out with the use of a Tauc plot, which was devised using the absorbance against wavelength data of CPs. The Lambda 750 UV/VIS/NIR Spectrometer, a PerkinElmer Corporation instrument, was utilized to obtain the absorbance against wavelength data.



Scheme 2. The possible coordination sites of linker H₃KL (a) and bifunctional ligand 4,4'-TMDP (b).

3. Result & discussions

3.1. FTIR

Fig. 1 shows that the FTIR spectra of Cu-CP demonstrate the presence of (O–H) stretch vibrations and (N–H) stretch vibrations within the range of 3400 cm^{-1} to 3200 cm^{-1} . The stretches that were detected at 3146 cm^{-1} , 1398 cm^{-1} , and 1016 cm^{-1} allow for an inference to be made about the existence of a benzene ring in the Cu-CP. The peak around at 1689 cm^{-1} and around at 1602 cm^{-1} area is attributed for the C=O and C=N bond respectively. The peaks in the range 1500 cm^{-1} to 1400 cm^{-1} attributed for the (C=N) and (C=C) bond of heterocyclic ring. Within the range of 3150 cm^{-1} to 3000 cm^{-1} in the spectrum, is attributed for the stretching vibration of C–H. The weak peaks in the finger print region at 501 cm^{-1} is attributed for the Cu–O or Cu–N bonding of Cu-CP [24].

The FTIR spectra of Zr-CP (as depicted in Fig. 1) revealed the presence of $\nu(\text{O–H})$ stretch vibrations and $\nu(\text{N–H})$ stretch vibrations within the range of 3600 cm^{-1} to 3300 cm^{-1} . The presence of a benzene ring in the Zr-CP is suggested by the observed stretches at 3109 cm^{-1} , 1388 cm^{-1} , and 1018 cm^{-1} . The presence of a robust frequency in the 1689 cm^{-1} range is indicative of the C=O functional group, while the peaks associated with the $\nu(\text{C=N})$ and $\nu(\text{C=C})$ stretch vibrations manifest within the 1650 cm^{-1} to 1500 cm^{-1} range. The stretching vibration of the $\nu(\text{C–H})$ bonds associated with the 4,4/TMDP ligand was detected within the spectral region of 3109 cm^{-1} to 3000 cm^{-1} . Additional peaks observed within the fingerprint region, such as the peak at 802 cm^{-1} , may indicate the presence of bonding between Zr and O or Zr and N [25].

3.2. Thermogravimetric analysis (TGA)

The thermal disintegration of both CPs was investigated by thermogravimetric analysis (TGA) and it was accomplished from room temperature to $550\text{ }^{\circ}\text{C}$. Both of them were burned under nitrogen atmosphere with a heating rate of $10\text{ }^{\circ}\text{C}/\text{min}$. Moreover, the thermal stability was calculated.

From Fig. 2, it can be seen that the Cu-CP showed thermal stability up to $270\text{ }^{\circ}\text{C}$, and for the Zr-CP, it was almost $315\text{ }^{\circ}\text{C}$. In there, some weight was lost due to some moisture and impurities, but the CPs were stable up to that maximum temperature. Specifically, for the Zr-CP, the sample was quite large, and it was 14.76 mg . As a result, the weight lost was significant up to its maximum stable temperature. At the maximum stable temperature of both CPs, 2.42% and 5.83% weight were lost for Cu-CP and Zr-CP, respectively. Fig. 3 represents the DSC of Cu-CP and Zr-CP. Furthermore, a compound is destroyed stepwise in TGA analysis. Firstly, the weak bonds in the compounds will be broken. Lastly, the extra stability that is formed by the strong bonds in the compounds will be broken. In this study, both CPs have not completely burned up to $550\text{ }^{\circ}\text{C}$. Consequently, only one step of burning would be observed. In this step, Cu-CP was rapidly burned (66.38% weight) up to $520\text{ }^{\circ}\text{C}$ and Zr-CP was burned (35.9% weight) almost linearly up to $550\text{ }^{\circ}\text{C}$.

3.3. Powder-XRD

Both of the CPs went through the process of having powder X-ray diffraction done on them. As can be seen in Fig. 4, the simulated pattern, which was taken from the SCXRD data, and the PXRD pattern of the synthesized CPs are very similar to one another. This finding provides an evidence for the high degree of purity possessed by both of the current CPs. The PXRD pattern indicates that both CPs have crystalline properties.

3.4. Band gap analysis

The UV–Visible absorption spectrum of CPs was collected at ambient environmental conditions at $25\text{ }^{\circ}\text{C}$. The light absorption

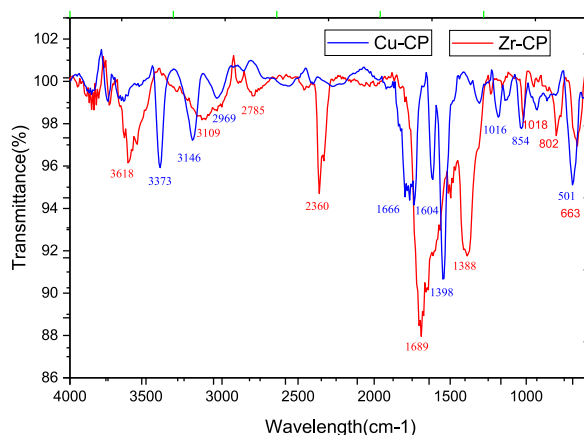


Fig. 1. Ftir spectrum of Cu-CP and Zr-CP

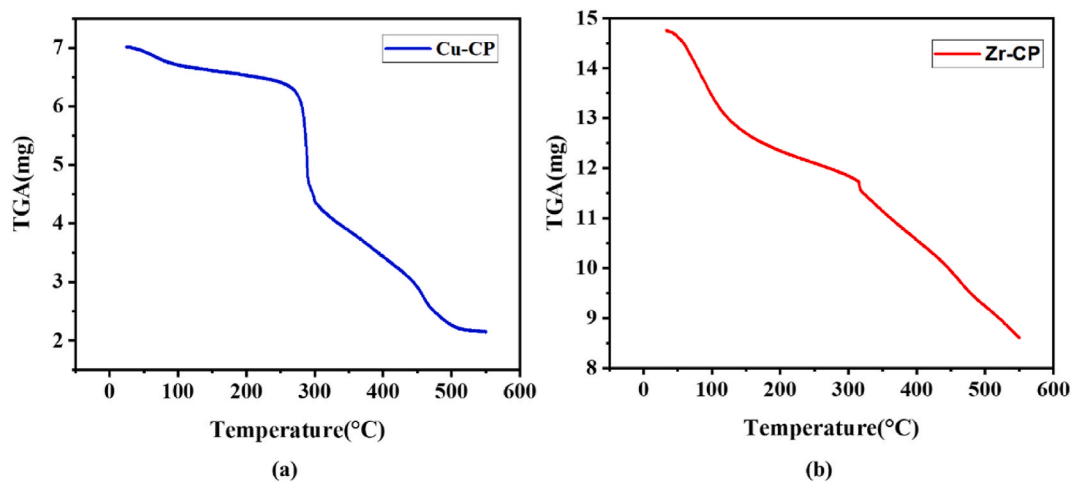


Fig. 2. TGA of Cu-CP (a) and Zr-CP (b).

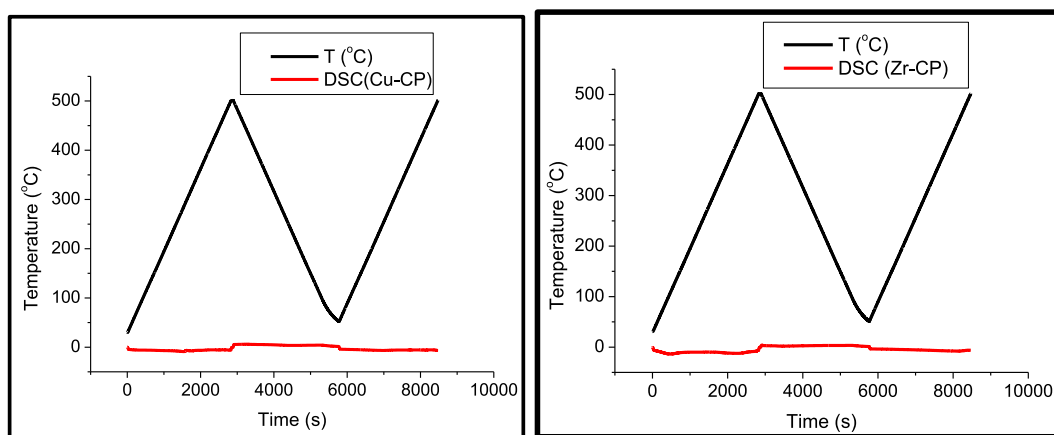


Fig. 3. Dsc of Cu-CP and Zr-CP

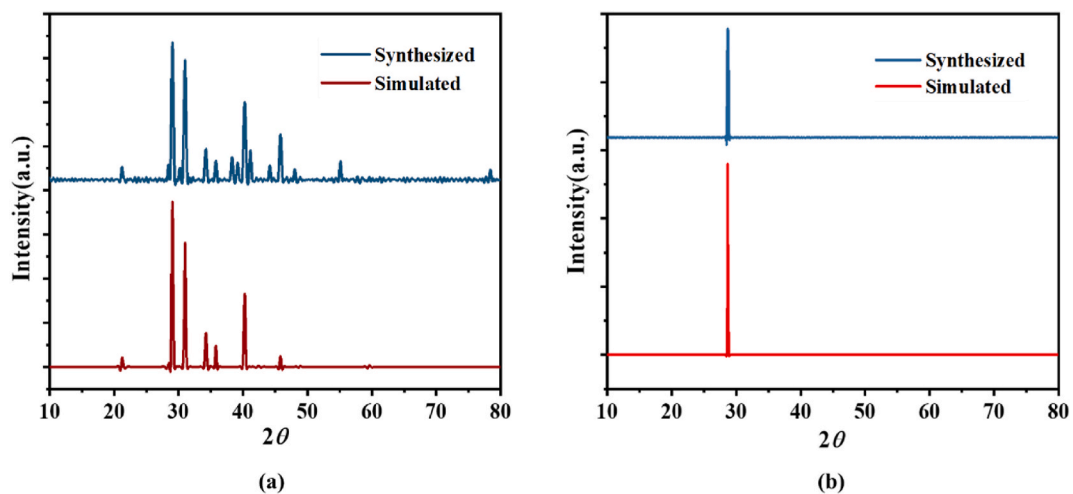


Fig. 4. X-ray crystallography of Cu-CP (a) and Zr-CP (b).

performance of CPs was analyzed in this study. From the absorbance against wavelength data, the calculated band gap of the CPs photocatalyst, as shown in Fig. 5, was determined and for Cu-CP it's to be 2.17 eV and for Zr-CP it's to be 2.2 eV by using the Tauc plot method where $n = 2$ for direct allowed transitions was used.

If the band gap is too low, there is a chance of recombining the valence band (VB) and conduction band (CB), and on the other hand, if the band gap is too large, higher energy is needed to transfer the electron from VB to CB which is not possible in sunlight or visible region. Finally, the conclusion is that the band gap should be optimum. In the literature point of view, the CPs have met the optimum band gap requirement [26–28]. The observed improvement in photo-response prompts further investigation into the photocatalytic behaviors of the material, as it has the potential to yield enhanced photocatalytic activity.

3.5. Scanning electron microscopy (SEM)

Scanning electron microscopy (SEM) analysis was used to comprehend the morphology of Cu-CP and Zr-CP. Both crystals' shape and texture are well-understood from the SEM images. These images (Figs. 6–7) provide abundant information about morphology. It is evident from the images that both crystals exhibit a polyhedral shape.

It is also clear that both crystals have good porosity. These pores play a vital role in the photocatalytic reaction by increasing the surface area.

3.6. Photocatalytic activity

The utilization of organic dyes in manufacturing and production has resulted in their classification as potent organic pollutants, thereby presenting a significant challenge to the environment. The present study focuses on the utilization of MB as a target organic dye to evaluate the photocatalytic efficacy of recently synthesized CPs under natural sunlight. The compound MB displays a characteristic maximum absorption at a wavelength of 664 nm, which can be detected through the employment of UV-visible spectrophotometric techniques when CPs are present. The degradation of the absorption spectra intensity of MB in an aqueous medium is observed to occur over varying time intervals upon irradiation in the presence of CPs. It is crucial to observe that the reduction in the magnitude of the absorption spectra is attributable to the absence of chromophore groups [29,30] that are responsible for their color changes. A control experiment was conducted under dark conditions in the absence of catalysts, which resulted in the absence of any significant alteration in the intensity of MB. The degradation of MB is significantly managed by CPs, whereas under dark conditions (Fig. 8), less significant changes are observed in the degradation of MB.

3.6.1. Effect of pH on the degradation property

pH is one of the most important parameters for the degradation of dye. As MB is a cationic dye the degradation was performed in without adding any pH-changing compound (Fig. 9), adding a buffer tablet to maintain pH at 9.2 (Fig. 10) and adding NaOH to maintain pH at 12 (Fig. 11). At the higher pH, more degradation happens, because of the formation of more OH radical. By analyzing all of the degradation curves from Fig. 5 the pH effect can be easily understood. In there, all conditions of MB dye degradation are nicely explained.

Without a catalyst (Blank), methylene blue was slowly degraded and the curve is almost linear, almost 20 % was degraded within 2 h. With catalyst in the dark condition was performed and there was very negligible degradation in Zr-CP and almost 7 % degradation in Cu-CP. Without adding any pH-changing compound not-so-well degradation curve was found in which 30 % of MB degradation was obtained by Cu-CP and 43 % for Zr-CP. At pH = 9.2, the almost exponential curve was found in which 62 % of MB degradation was obtained by Cu-CP and 72 % by Zr-CP (Fig. 12). At the pH = 12 exponential curve was found in which MB almost degraded. It can be

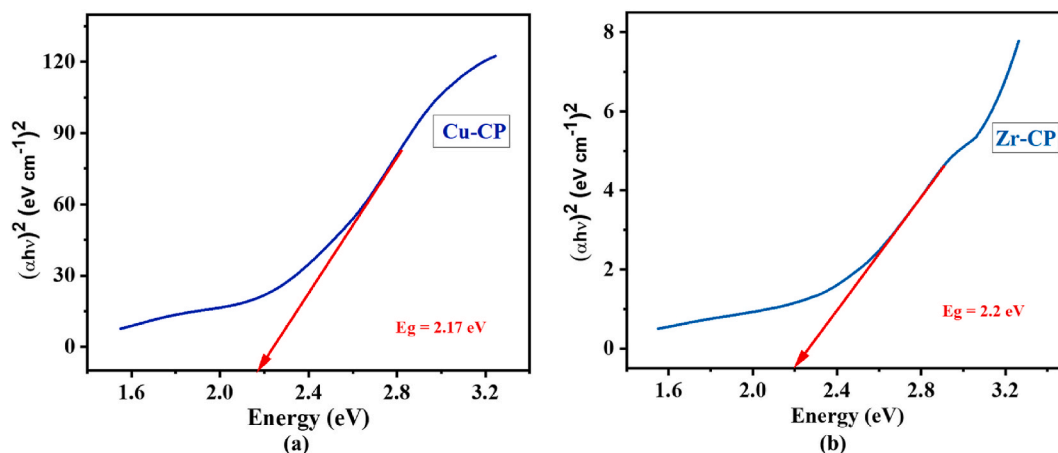


Fig. 5. The Tauc plot of Cu-CP (a) and Zr-CP (b).

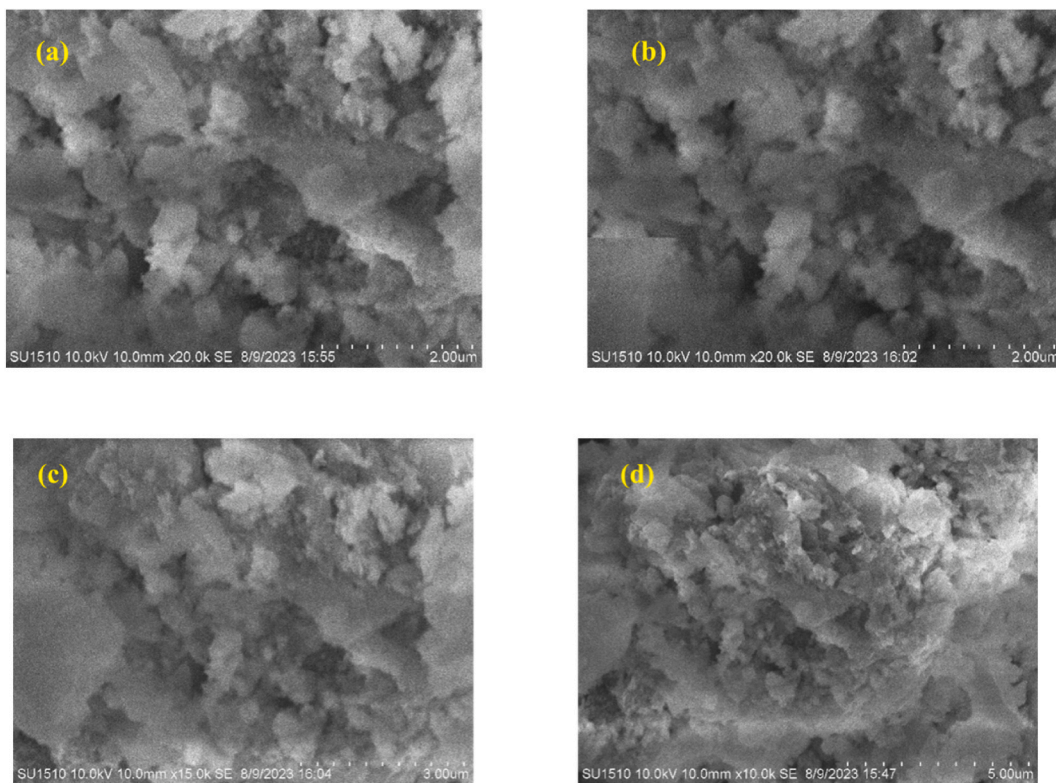


Fig. 6. SEM images of Cu-CP

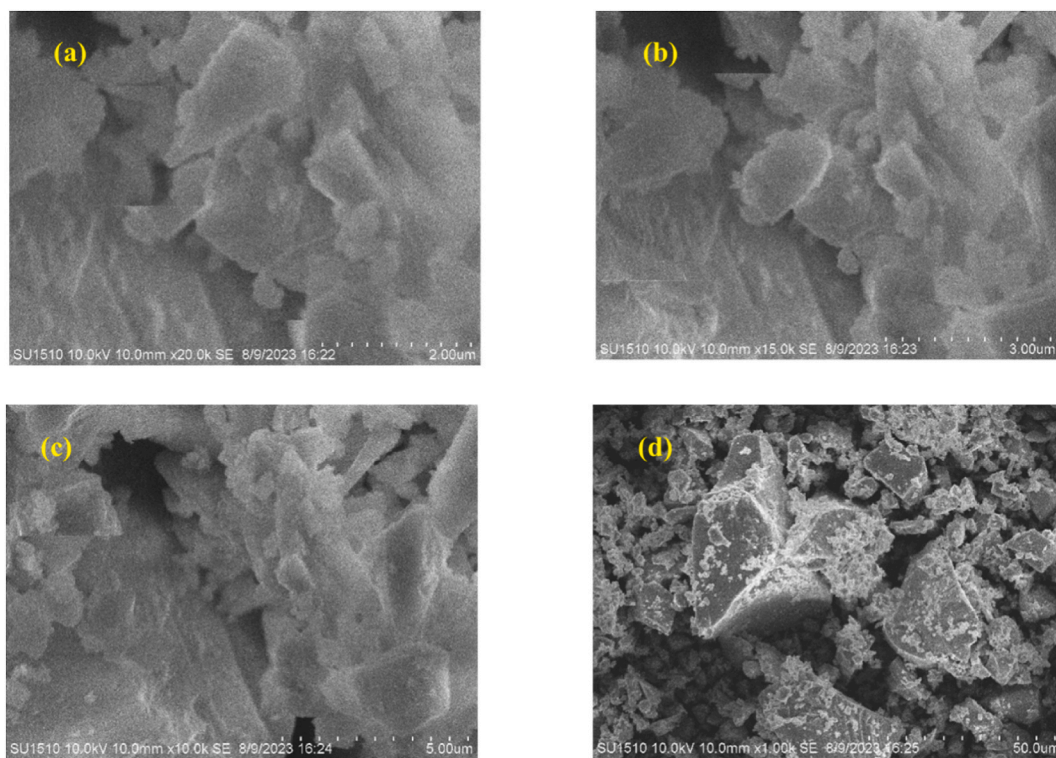


Fig. 7. SEM images of Zr-CP

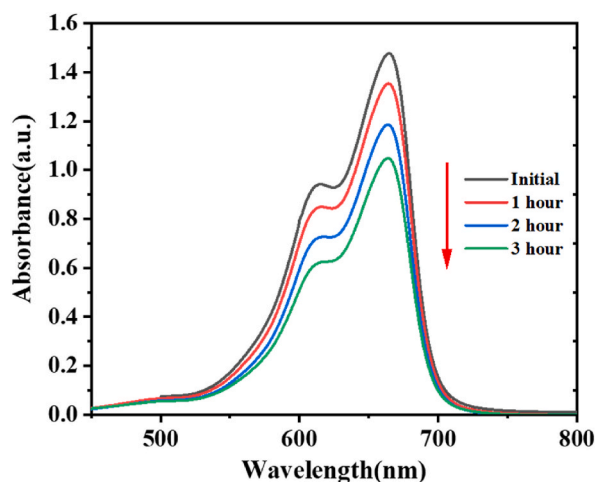


Fig. 8. The degradation of methylene blue (MB) without catalyst under sunlight at different time. (For interpretation of the references to color in this figure legend, the reader is referred to the Web version of this article.)

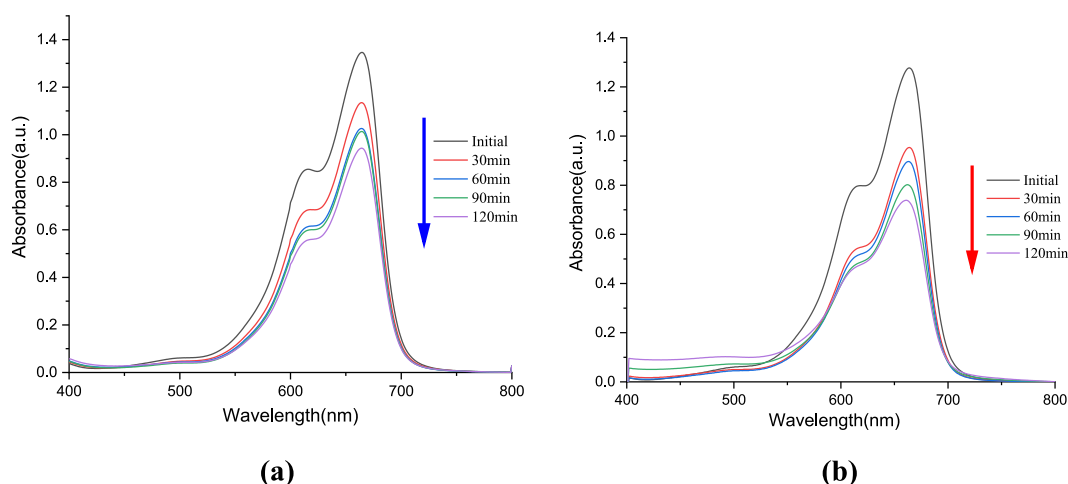


Fig. 9. The degradation of methylene blue (MB) at pH 7.3 in presence of Cu-CP (a) and Zr-CP (b). (For interpretation of the references to color in this figure legend, the reader is referred to the Web version of this article.)

concluded that pH is a vital issue for the degradation but not only pH but also other factors most importantly the band gap is also a vital issue. The intensity of sunlight also played an important role, the intensity was approximately 200 W m^{-2} in the observation month was October. So, all of these were the main considerations for the high-level degradation of MB.

3.6.2. Photocatalytic mechanism

The Zr/Cu-CP photocatalytic reaction can be elucidated through the principles of semiconductor theory, as depicted in Fig. 13. Specifically, when the level of material absorption is equal to or greater than the photon energy of its forbidden bandwidth, the electrons located in the valence band become excited and transition to the conduction band, resulting in the creation of photogenic electrons in the conduction band and photogenic holes in the valence band. Photogenic holes have been identified as potent oxidizing agents that can cause direct degradation of the structure of MB that has been previously adsorbed on the surface of the catalyst. Additionally, these holes can react with H_2O or OH^- present in the solution to generate $\cdot\text{OH}$ radicals that possess exceptional oxidation capabilities. Electrons generated through photochemical processes exhibit reductive properties and have the potential to engage in a reaction with oxygen molecules present in a solution, resulting in the formation of $\cdot\text{O}_2^-$ radical³¹. The photocatalytic process involving photogenic holes (h^+), $\cdot\text{OH}$ and $\cdot\text{O}_2^-$ radicals plays a key role in the oxidation reactions (Fig. 12). These oxidants selectively degrade organic compounds into non-toxic and harmless small molecules such as Cl^- , NO_3^- , H_2O , CO_2 , etc. The major products are H_2O and CO_2 . The Zr/Cu-CP photocatalyst is employed in this process. The synthesized coordination polymers perform as potential photocatalysts for two main reasons. Firstly, it shows the required band gap to perform as a photocatalyst, secondly, the structure of coordination polymer has conjugated double bonds, so the photogenic hole (h^+) and electrons get the required time to initiate the

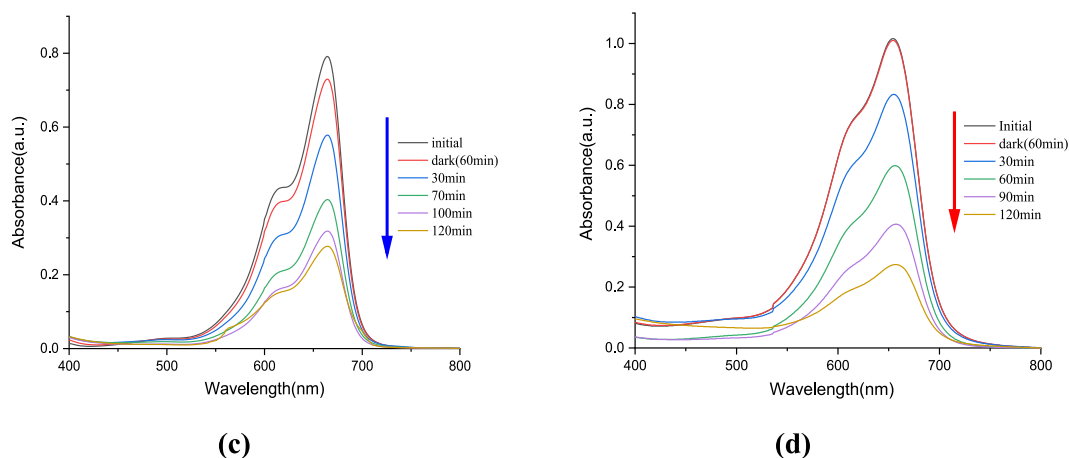


Fig. 10. The degradation of methylene blue (MB) at pH 9.2 in presence of Cu-CP (c) and Zr-CP (d). (For interpretation of the references to color in this figure legend, the reader is referred to the Web version of this article.)

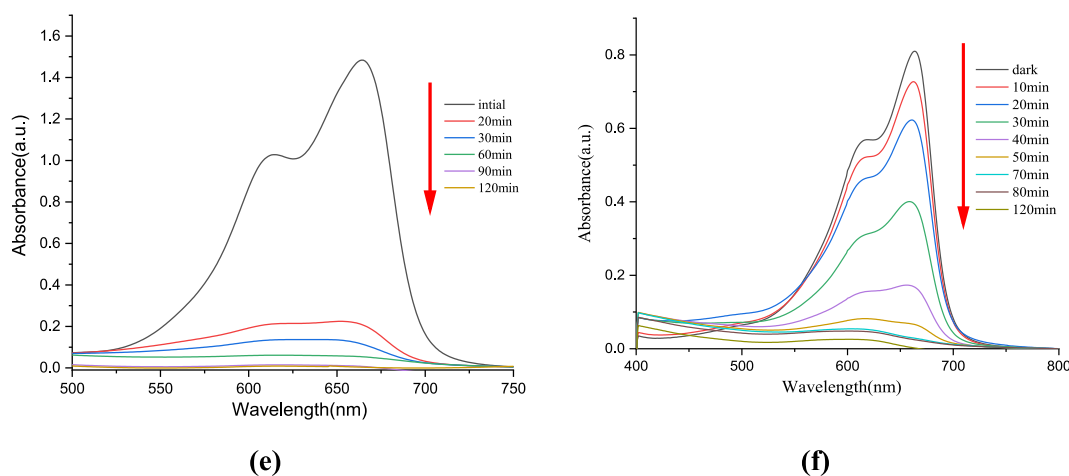


Fig. 11. The degradation of methylene blue (MB) at pH 12.0 in presence of Cu-CP (e) and Zr-CP (f). (For interpretation of the references to color in this figure legend, the reader is referred to the Web version of this article.)

degradation rather than immediate coupling.

3.7. The reusability and stability test

The coordination polymer Cu-CP and Zr-CP is very stable. The photocatalyst is heterogeneous, so it can be easily collected for reusing. The FTIR spectra (Fig. 14) of the coordination polymer after reuse was observed. There no significant change was found, so it indicates the stability and recyclability of these coordination polymers.

4. Conclusion

In brief, a pair of innovative coordination polymers, namely Zr-CP and Cu-CP, were successfully synthesized through a hydrothermal method. The absorption of sunlight is utilized for the purpose of photocatalytic reactions. The results indicate that the degradation of MB was most effectively achieved by both CPs under basic conditions with a pH of 12. The utilization of both CPs as catalysts for the photocatalytic degradation of MB wastewater has been found to yield nontoxic colorless smaller species as the final product. This process effectively reduces the likelihood of the formation of various organic intermediates. The present study focuses on exploring the photocatalytic activity of CPs, which may provide a novel approach for the eco-friendly degradation of pesticide-contaminated wastewater. These materials are considered as an optimal alternative to semiconductor materials.

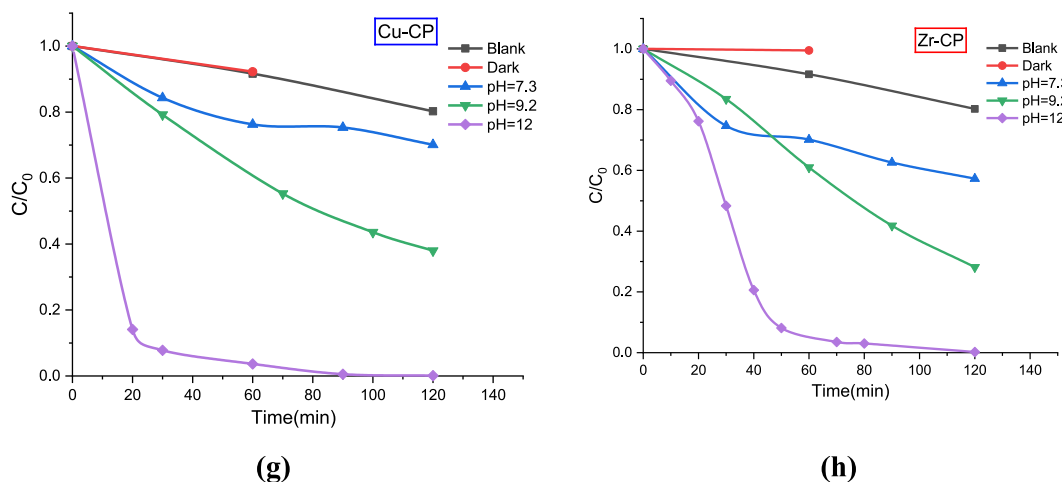


Fig. 12. The variation of degradation of methylene blue (MB) concentration under various conditions in the presence of photocatalyst Cu-CP (g) and Zr-CP (h). (For interpretation of the references to color in this figure legend, the reader is referred to the Web version of this article.)

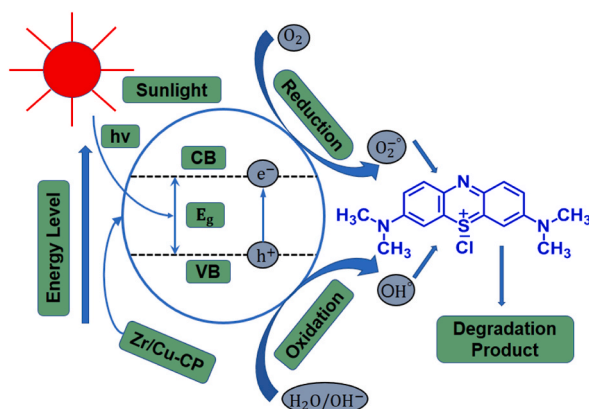


Fig. 13. Photocatalytic degradation mechanism of dye.

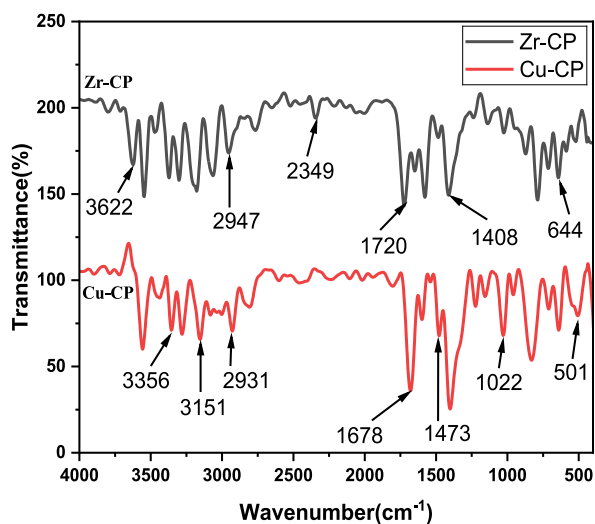


Fig. 14. The FTIR of recycled photocatalyst Cu-CP and Zr-CP

Data availability statement

Data will be made available on request.

CRediT authorship contribution statement

Md Mohibul Alam: Writing – review & editing, Visualization, Funding acquisition, Data curation. **Md. Foysal Ahmed:** Writing – review & editing, Visualization, Project administration, Investigation, Formal analysis, Data curation. **Md. Azharul Arafath:** Writing – review & editing, Writing – original draft, Supervision, Project administration, Methodology, Investigation, Funding acquisition, Formal analysis, Conceptualization. **Mohammad Razaul Karim:** Validation, Software, Resources. **Md Nizam Uddin:** Writing – review & editing, Visualization, Software, Resources. **Md Sohrab Hossain:** Validation, Software, Resources, Formal analysis, Data curation.

Declaration of competing interest

There are no conflicts of interest to declare.

Acknowledgment

The authors wish to thank Research Center, Shahjalal University of Science and Technology, Sylhet 3114, Bangladesh for Promotional Research Grant Project ID: PS/2023/1/04 and Advance Research Grant Project ID: AS/2021/1/12.

References

- [1] D. Shen, J. Fan, W. Zhou, B. Gao, Q. Yue, Q. Kang, Adsorption kinetics and isotherm of anionic dyes onto organo-bentonite from single and multisolute systems, *J. Hazard Mater.* 172 (2009) 99–107.
- [2] W.-J. Ong, L.-L. Tan, Y.H. Ng, S.-T. Yong, S.-P. Chai, Graphitic carbon nitride (g-C₃N₄)-based photocatalysts for artificial photosynthesis and environmental remediation: are we a step closer to achieving sustainability? *Chem. Rev.* 116 (2016) 7159–7329.
- [3] M. Zhou, H. Yang, T. Xian, R.S. Li, H.M. Zhang, X.X. Wang, Sonocatalytic degradation of RhB over LuFeO₃ particles under ultrasonic irradiation, *J. Hazard Mater.* 289 (2015) 149–157.
- [4] Y. He, H. Lv, Y. Daili, Q. Yang, L.B. Junior, D. Liu, H. Liu, Z. Ma, Construction of a new cascade photogenerated charge transfer system for the efficient removal of bio-toxic levofloxacin and rhodamine B from aqueous solution: mechanism, degradation pathways and intermediates study, *Environ. Res.* 187 (2020) 109647.
- [5] A. Mariyam, M. Shahid, M. I. M.S. Khan, M.S. Ahmad, Tetrazole based porous metal organic framework (MOF): topological analysis and dye adsorption properties, *J. Inorg. Organomet. Polym. Mater.* 30 (2020) 1935–1943.
- [6] M.S. Khan, M. Khalid, M.S. Ahmad, M. Shahid, M. Ahmad, Three-in-one is really better: exploring the sensing and adsorption properties in a newly designed metal–organic system incorporating a copper (II) ion, *Dalton Trans.* 48 (2019) 12918–12932.
- [7] S.-S. Chen, Z.-Y. Zhang, R.-B. Liao, Y. Zhao, C. Wang, R. Qiao, Z.-D. Liu, A photoluminescent Cd (II) coordination polymer with potential active sites exhibiting multiresponsive fluorescence sensing for trace amounts of NACs and Fe³⁺ and Al³⁺ ions, *Inorg. Chem.* 60 (2021) 4945–4956.
- [8] Z. Liu, Z. Yang, T. Li, B. Wang, Y. Li, D. Qin, M. Wang, M. Yan, An effective Cu (II) quenching fluorescence sensor in aqueous solution and 1D chain coordination polymer framework, *Dalton Trans.* 40 (2011) 9370–9373.
- [9] M.M. Deshmukh, M. Ohba, S. Kitagawa, S. Sakaki, Absorption of CO₂ and CS₂ into the Hofmann-type porous coordination polymer: electrostatic versus dispersion interactions, *J. Am. Chem. Soc.* 135 (2013) 4840–4849.
- [10] J.T. Culp, L. Sui, A. Goodman, D. Luebke, Carbon dioxide (CO₂) absorption behavior of mixed matrix polymer composites containing a flexible coordination polymer, *J. Colloid Interface Sci.* 393 (2013) 278–285.
- [11] J.M. Seco, I. Oyarzabal, S. Perez-Yanez, J. Cepeda, A. Rodriguez-Dieguez, Designing multifunctional 5-cyanoisophthalate-based coordination polymers as single-molecule magnets, adsorbents, and luminescent materials, *Inorg. Chem.* 55 (2016) 11230–11248.
- [12] Y.-Z. Zheng, Z. Zheng, X.-M. Chen, A symbol approach for classification of molecule-based magnetic materials exemplified by coordination polymers of metal carboxylates, *Coord. Chem. Rev.* 258 (2014) 1–15.
- [13] Y. Chen, M. Tang, Y. Wu, X. Su, X. Li, S. Xu, S. Zhuo, J. Ma, D. Yuan, C. Wang, A one-dimensional π -d conjugated coordination polymer for sodium storage with catalytic activity in Negishi coupling, *Angew. Chem. Int. Ed.* 58 (2019) 14731–14739.
- [14] C. Li, X. Yin, L. Chen, Q. Li, T. Wang, Synthesis of cobalt ion-based coordination polymer Nanowires and their Conversion into porous Co₃O₄ nanowires with good lithium storage properties, *Chem.–Eur. J.* 16 (2010) 5215–5221.
- [15] X. Yin, L.-P. Lv, X. Tang, X. Chen, W. Sun, Y. Wang, Designing cobalt-based coordination polymers for high-performance sodium and lithium storage: from controllable synthesis to mechanism detection, *Mater. Today Energy* 17 (2020) 100478.
- [16] W.J. Rieter, K.M. Pott, K.M.L. Taylor, W. Lin, Nanoscale coordination polymers for platinum-based anticancer drug delivery, *J. Am. Chem. Soc.* 130 (2008) 11584–11585.
- [17] Z. Ma, B. Moulton, Recent advances of discrete coordination complexes and coordination polymers in drug delivery, *Coord. Chem. Rev.* 255 (2011) 1623–1641.
- [18] H. Yao, F. Zhang, G. Zhang, H. Luo, L. Liu, M. Shen, Y. Yang, A novel two-dimensional coordination polymer-polypyrrole hybrid material as a high-performance electrode for flexible supercapacitor, *Chem. Eng. J.* 334 (2018) 2547–2557.
- [19] D. Chen, F. Liang, D. Feng, M. Xian, H. Zhang, H. Liu, F. Du, An efficient route from reproducible glucose to 5-hydroxymethylfurfural catalyzed by porous coordination polymer heterogeneous catalysts, *Chem. Eng. J.* 300 (2016) 177–184.
- [20] Y.-B. Huang, Q. Wang, J. Liang, X. Wang, R. Cao, Soluble metal-nanoparticle-decorated porous coordination polymers for the homogenization of heterogeneous catalysis, *J. Am. Chem. Soc.* 138 (2016) 10104–10107.
- [21] Z. Zhou, C. He, L. Yang, Y. Wang, T. Liu, C. Duan, Alkyne activation by a porous silver coordination polymer for heterogeneous catalysis of carbon dioxide cycloaddition, *ACS Catal.* 7 (2017) 2248–2256.
- [22] M.S. Khan, M. Khalid, M. Shahid, A Co (II) coordination polymer derived from pentaerythritol as an efficient photocatalyst for the degradation of organic dyes, *Polyhedron* 196 (2021) 114984.
- [23] Z.-Z. Xue, Q.-W. Guan, L. Xu, X.-D. Meng, J. Pan, A Zn (II)-based coordination polymer featuring selective detection of Fe³⁺ and efficient capture of anionic dyes, *Cryst. Growth Des.* 20 (2020) 7477–7483.
- [24] L. Debbichi, M.C. Marco de Lucas, J.F. Pierson, P. Kruger, Vibrational properties of CuO and Cu₂O from first-principles calculations, and Raman and infrared spectroscopy, *J. Phys. Chem. C* 116 (2012) 10232–10237.

- [25] S.B. Patel, N. Baker, I. Marques, A. Hamlekhan, M.T. Mathew, C. Takoudis, C. Friedrich, C. Sukotjo, T. Shokuhfar, Transparent TiO₂ nanotubes on zirconia for biomedical applications, *RSC Adv.* 7 (2017) 30397–30410.
- [26] T.M. Breault, B.M. Bartlett, Lowering the band gap of anatase-structured TiO₂ by coalloying with Nb and N: electronic structure and photocatalytic degradation of methylene blue dye, *J. Phys. Chem. C* 116 (2012) 5986–5994.
- [27] A. Ghafoor, I. Bibi, S. Ata, F. Majid, S. Kamal, M. Iqbal, S. Iqbal, S. Noureen, B. Basha, N. Alwadai, Energy band gap tuning of LaNiO₃ by Gd, Fe and Co ions doping to enhance solar light absorption for efficient photocatalytic degradation of RhB dye: a mechanistic approach, *J. Mol. Liq.* 343 (2021) 117581.
- [28] D. Das, R.K. Dutta, A novel method of synthesis of small band gap SnS nanorods and its efficient photocatalytic dye degradation, *J. Colloid Interface Sci.* 457 (2015) 339–344.
- [29] M. Choura, N.M. Belgacem, A. Gandini, Acid-catalyzed polycondensation of furfuryl alcohol: mechanisms of chromophore formation and cross-linking, *Macromolecules* 29 (1996) 3839–3850.
- [30] A. Gürses, M. Açıkyıldız, K. Güneş, M.S. Gürses, A. Gürses, M. Açıkyıldız, K. Güneş, M.S. Gürses, Dyes and pigments: their structure and properties, *Dyes Pigments* (2016) 13–29.